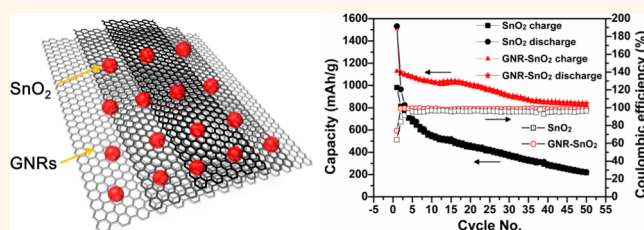# Graphene Nanoribbon and Nanostructured SnO$_2$ Composite Anodes for Lithium Ion Batteries

Jian Lin,[†,‡] Zhiwei Peng,[§] Changsheng Xiang,[§] Gedeng Ruan,[§] Zheng Yan,[§] Douglas Natelson,[⊥,∥,*] and James M. Tour[†,‡,§,#,*]

[†]Department of Mechanical Engineering and Material Science; [‡]Smalley Institute for Nanoscale Science. & Technology; [§]Department of Chemistry; [⊥]Department of Physics and Astronomy; [∥]Department of Electrical and Computer Engineering; [#]Department of Computer Science, Rice University, 6100 Main Street, Houston, Texas 77005, United States

ABSTRACT A composite made from graphene nanoribbons (GNRs) and tin oxide (SnO$_2$) nanoparticles (NPs) is synthesized and used as the anode material for lithium ion batteries (LIBs). The conductive GNRs, prepared using sodium/potassium unzipping of multiwall carbon nanotubes, can boost the lithium storage performance of SnO$_2$ NPs. The composite, as an anode material for LIBs, exhibits reversible capacities of over 1520 and 1130 mAh/g for the first discharge and charge, respectively, which is more than the theoretical capacity of SnO$_2$. The reversible capacity retains ∼825 mAh/g at a current density of 100 mA/g with a Coulombic efficiency of 98% after 50 cycles. Further, the composite shows good power performance with a reversible capacity of ∼580 mAh/g at the current density of 2 A/g. The high capacity, good power performance and retention can be attributed to uniformly distributed SnO$_2$ NPs along the high-aspect-ratio GNRs. The GNRs act as conductive additives that buffer the volume changes of SnO$_2$ during cycling. This work provides a starting point for exploring the composites made from GNRs and other transition metal oxides for lithium storage applications.

KEYWORDS: graphene nanoribbons · GNRs · SnO$_2$ · lithium ion batteries · capacity

The development of new anode materials with high specific capacity for lithium-ion batteries (LIBs) is a key step forwarded for applications to large-scale energy storage units such as electrical vehicles.[1,2] Graphite, the standard commercialized anode material for LIBs, has a theoretical specific capacity of only 372 mAh/g,[3] which limits its applications in LIBs. Therefore, new anode materials with high specific capacity such as Si (4200 mAh/g), Sn (994 mAh/g), and SnO$_2$ (782 mAh/g) have been intensively investigated.[4−6] However, the enormous volume expansion and structural changes during repeated alloying/dealloying causes significant capacity fading during cycling.[4,7] To address this problem, researchers have employed several approaches. One tactic is the development of electrode materials based upon nanostructures that minimize the strain during volume expansion.[8,9] Another approach is to integrate the electrode material with a carbonaceous matrix such as amorphous carbon,[5] mesoporous carbon,[7] graphene,[6,10−12] or carbon nanotubes (CNTs).[13,14]

Graphene nanoribbons (GNRs), a quasi-one-dimensional form of graphene, exhibit tunable electrical properties through dimension confinement[15,16] as well as edge morphology[17] or functionalization.[18] Interestingly, GNRs have been theoretically[19] and experimentally[20] shown to enhance lithium storage through edge effects. Moreover, GNRs, having large aspect ratios and high surface area, might provide an excellent conductive matrix with good mechanical flexibility for the metal oxide to accommodate the volume changes during change/discharge cycles. Here, we used our recently developed conductive GNRs to prepare anode composite materials with SnO$_2$ nanoparticles (NPs) for LIBs. The SnO$_2$ NPs were synthesized *via* a simple chemical method, with a size of ∼10 nm, and they were uniformly distributed among the GNR structure layers. The GNRs were made by Na/K unzipping of MWCNTs. The fabricated anode based on the GNR/SnO$_2$ composite exhibited a specific reversible capacity over 1130 mAh/g. Moreover, using sodium carboxymethylcellulose

(Na-CMC) as the binder material affords an enhanced cyclability to the GNR/SnO$_2$ anode. The reversible capacity retains a specific capacity of ~825 mAh/g at current density of 100 mA/g with Coulombic efficiency of 98.3% after 50 cycles. The composite also shows good power performance with a reversible capacity of ~580 mAh/g at a current density of 2 A/g.

RESULTS AND DISCUSSION

The synthesis of the GNRs/SnO$_2$ composite is illustrated in Figure 1. First, the GNRs were obtained using
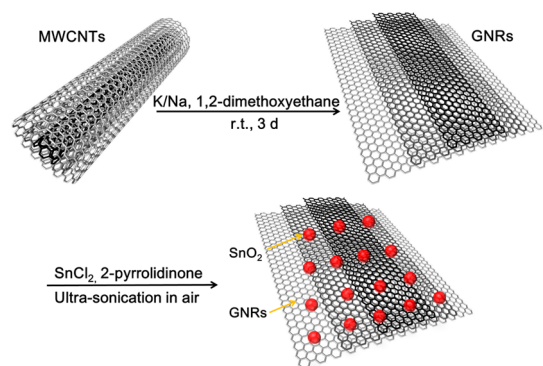

Figure 1. Scheme for the synthesis of the GNRs/SnO$_2$ composite.

K/Na alloy to unzip the MWCNTs.[21,22] Then, SnCl$_2$ and 2-pyrrolidinone were added into the GNRs with ultra-sonication for reducing Sn^{2+} to Sn^0. Lastly, the Sn NPs were oxidized overnight using ultrasonication in air. The morphology of the obtained GNRs/SnO$_2$ composites was characterized with SEM. Figure 2a is the SEM image of GNRs after unzipping, showing that the width of GNRs is ~200 nm. The SEM image of the GNRs/SnO$_2$ composite (Figure 2b) shows that SnO$_2$ NPs are dispersed among the entangled GNRs, with some aggregation. From the TEM image (Figure 2c), most of the SnO$_2$ NPs are <10 nm and are uniformly distributed along the GNRs. The HRTEM analysis exhibits the lattice fringe, indicative of single crystal SnO$_2$ (Figure 2d). The spacing of the adjacent lattice planes is 0.339 nm, agreeing well with the (110) plane of rutile SnO$_2$.[23] The GNRs have an average of 15 graphene layers with indicative lattice spacing of 0.338 nm.

Figure 3a exhibits the XRD pattern from the as-prepared GNRs/SnO$_2$ composite. The characteristic peak of GNRs was observed from the diffraction pattern. The indexed peaks of SnO$_2$ correspond to the tetragonal rutile structure of SnO$_2$ with lattice constants of a = 0.4721 nm and c = 0.3215 nm. The calculated particle size using the Scherrer formula is ~7 nm,[24] in good agreement with the results from TEM analysis. XPS analysis was conducted to further confirm
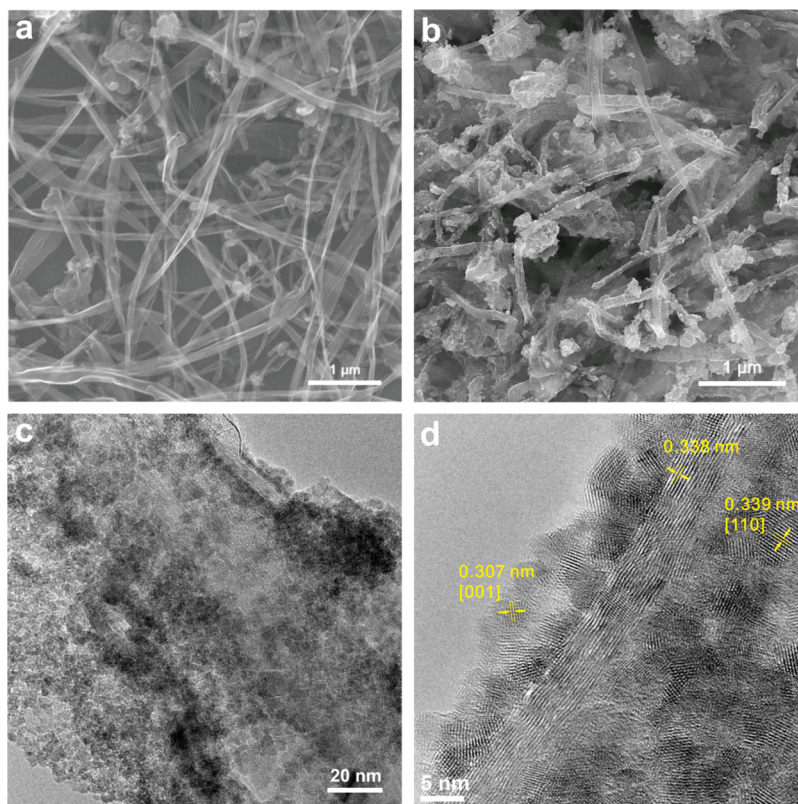

Figure 2. SEM and TEM images of the GNRs/SnO$_2$ composite. (a) SEM image of the unzipped GNRs. (b) SEM image of the GNRs/SnO$_2$ composite. (c) TEM image of the composite showing SnO$_2$ NPs with sizes from ~4 to 10 nm that are uniformly distributed along the GNR structures. (d) HRTEM image of the composite, showing the graphitic structure of GNRs and the crystal structure of SnO$_2$ NPs.

the constituent phase of the as-prepared composite (Figure 3b). From the XPS spectrum, Sn, O and C are detected in the composite. The composite shows carbon atomic concentration of 54.2%, corresponding to a carbon content of 18.8 wt %. The TGA measurement was carried out in air (Figure 3c). From the TGA curve, GNRs/SnO$_2$ has 19.5% weight loss from 278 to 700 °C that can be assigned to combustion of GNRs in air, forming CO$_2$. This carbon weight loss agrees well with the result from XPS analysis. This indicates that the weight content of the SnO$_2$ in the composite is ~80%.

The choice of binder for the anode material plays an important role to enhance the specific capacity and cyclability in LIBs research. Polyvinylidene fluoride (PVDF) is the most commonly used binder material. Recently, water-soluble binder materials such as Na-CMC, poly(acrylic acid) (PAA) and polyvinyl acids (PVA) have been used in Si-based LIBs, producing enhanced electrochemical performance.[25−27] In a previous study, Na-CMC had been shown to enhance the cyclability of SnO$_2$-based anode materials;[28] thus, Na-CMC was employed as the binding material for our batteries. Cyclic voltammetry (CV) measurements were carried out to characterize the electrochemical behavior of the GNRs/SnO$_2$ composite as the anode material from 0.01 to 2.5 V with a scan rate of 0.5 mV/s. The CV curves of the initial three cycles are shown in Figure 4a. In the first cathodic sweep process, the irreversible broad peak (a) at ~0.7 V is attributed to the formation of a solid electrolyte interphase and decomposition of SnO$_2$ to form Sn.[29−32] The peak (a) disappears in the following cycles; it becomes a reversible peak (a′) at ~0.9 V indicating the formation of various Li$_x$Sn species that are reported by others.[11,29,31] The characteristic peak (b) at ~0.1 V in the first cathodic sweep process is associated with the alloying of Sn with Li. This peak was slightly shifted in subsequent scans and then stabilized at ~0.2 V. During the anodic sweep process, two peaks (c and d) at ~0.63 and ~1.35 V are observed. The characteristic peak at 0.63 V represents the dealloying process of Li$_x$Sn, while the peak at 1.35 V is thought to be related to the partially reversible reaction of SnO$_2$ with Li$^+$.[29,32,33] After the first cycle, all the CV curves are almost identical, thereby showing the reversibility of the composite electrode charge/discharge process.

The galvanostatic charge/discharge measurements were performed at the current density of 100 mA/g in the potential window of 0.01−2.5 V vs Li$^+$/Li. The given specific capacity was calculated based on the total mass of the GNRs/SnO$_2$ composite. The typical charge/discharge curves in first, second and 30th cycle are shown in Figure 4b. The composite can deliver a capacity of 1519 mAh/g for the first discharge and a reversible capacity of 1129 mAh/g. The irreversibility could be caused by the formation of a solid electrolyte interphase (SEI) as indicated from the CV curve of the
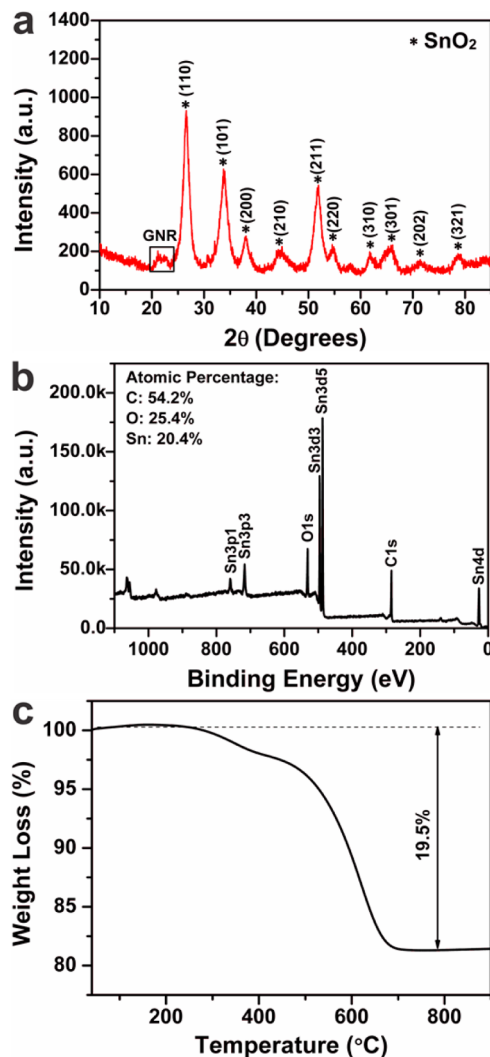

Figure 3. (a) XRD pattern of the GNRs/SnO$_2$ composite. The particle size estimated using the Scherrer equation was ~7 nm. (b) XPS spectrum of the GNRs/SnO$_2$ composite with the inset showing the atomic percentage of the carbon, tin and oxygen. The atomic percentage was obtained from high resolution scans. (c) TGA of the GNRs/SnO$_2$ composite in air. Samples were pretreated at 120 °C to dehydrate them prior to the measurement.

first cycle.[12] It shows the second discharge and charge capacities of 1116 and 1106 mAh/g, which is indicative of the high reversibility. The theoretical lithium capacity from SnO$_2$ is ~782 mAh/g based on the conventional alloying mechanism.[5] Here, the enhanced lithium storage capacity from the composite implies that there exists more lithium insertion/extraction sites in the composite, similar to reports in the reduced graphene oxide and tin dioxide (RGO/SnO$_2$) anodes.[11] There may also be a contribution from enhanced surface electrochemistry in nanocrystalline SnO$_2$.[34] The retention of the charge/discharge curves at the 50th cycle shows the stability of the composite as an anode material. The capacity retention performance of the GNRs/SnO$_2$ composite is shown in the Figure 4c. The specific capacity starts to stabilize at ~840 mAh/g after 40 cycles.
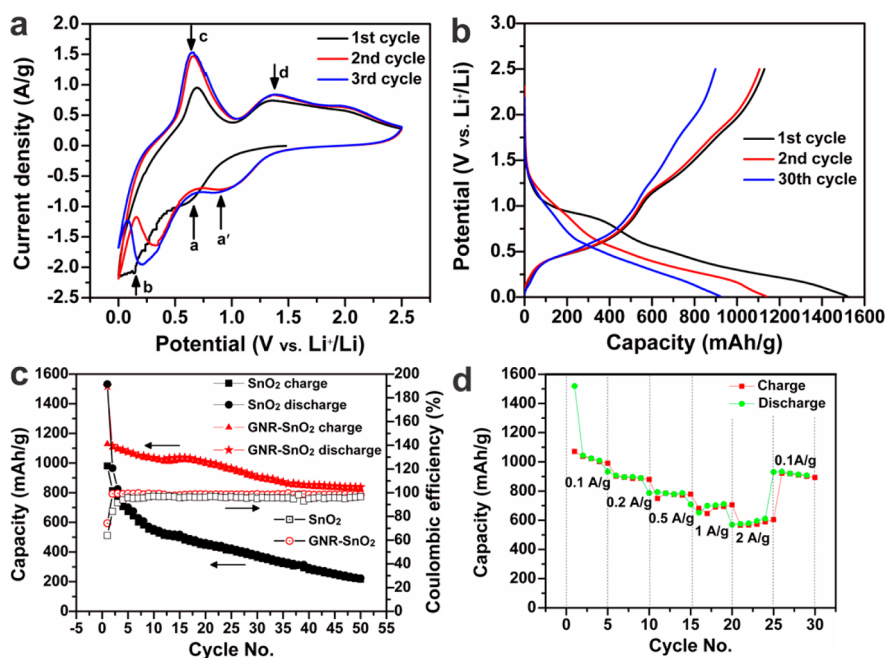
Figure 4. The electrochemical performance of the GNRs/SnO$_2$ composite electrodes. The specific capacities are calculated based on the total mass of the GNRs/SnO$_2$ composite in the anode electrodes. (a) CV curves of the first, second and third cycles of the composite electrodes at a scan rate of 0.5 mV/s over the voltage range of 0.01−2.5 V. (b) The first, second and 30th charge/discharge curves of the composite electrode at a rate of 100 mA/g. (c) Comparison of capacity retention and Coulombic efficiency of GNRs and the GNRs/SnO$_2$ composite at a rate of 100 mA/g. (d) Rate capability of the composite electrodes with various current densities.

Furthermore, the anode maintains a reversible discharge capacity of 825 mAh/g after 50 cycles, which is higher than that reported RGO/SnO$_2$-based anodes[10−12,35] and much higher than other SnO$_2$ and carbon based composites.[5,9,13] The Coulombic efficiency of the first cycle was 74.3%, but was above 98% after the second cycle and stayed at 98.3% after 50 cycles, indicating good capacity retention. As shown in Figure 4c, the reversible capacity of the GNRs/SnO$_2$ composite anode is much higher than that of the bare GNRs with reversible specific capacity of ∼250 mAh/g (Figure S1). In addition, the reversible specific capacity of SnO$_2$ NPs, a control sample composite prepared without GNRs, quickly degraded to ∼200 mAh/g after 50 cycles (Figure 4c), which indicates the significant effect that GNRs play in the composite.

The rate capability of the GNRs/SnO$_2$ composite was also evaluated by applying various current densities from 0.1 to 2 A/g (Figure 4d). The GNRs/SnO$_2$ composite anode exhibited high reversible capacities of ∼1010, ∼900, ∼780, ∼700, and ∼580 mAh/g at current densities of 0.1, 0.2, 0.5, 1, and 2 A/g, respectively. After 25 cycles at different current densities, when the current density was returned to the 0.1 A/g, the reversible capacity can be recovered to ∼930 mAh/g, which is close to the original value. To gain additional insight, the electrochemical impedance of the GNRs/SnO$_2$ composite anode electrode after 50 cycles was measured (Figure S2). The typical high-frequency and

low-frequency relaxation loops can be observed. By fitting the Nyquist plot with the Randles equivalent circuit, the low surface SEI resistance formed by the electrode was ∼38 Ω, which contributes to the high rate performance.[36] The highly reversible rate capacity can be attributed to the conductive GNR networks with large aspect ratios as well as the homogeneous distribution of small-sized SnO$_2$ nanoparticles along or between GNR stacks. The conductive GNRs network might further facilitate electrolyte diffusion and Li$^+$ transport into the nanosized SnO$_2$. The GNR networks act as conductive mechanical buffers, apparently able to adjust as needed to the volume change of SnO$_2$ during the cycling.

CONCLUSION

High-performance LIB composite anodes were successfully synthesized via uniformly distributing SnO$_2$ nanoparticles along or within the conductive GNR stacks. The obtained composite shows a high reversible discharge capacity of 1130 mAh/g and retains ∼825 mAh/g at the 50th cycle for current densities of 0.1 A/g. In addition, the composite exhibits excellent power capability, delivering a specific capacity of 580 mAh/g at a current density of 2 A/g, which is much higher than the theoretic capacity of graphite (372 mAh/g). The improved electrochemical performance may arise from the high aspect ratio GNRs with their conductive paths, which at the same time could serve as a mechanical buffer for SnO$_2$ NPs

expansion and contraction. The fabrication procedures for both GNRs and SnO$_2$ NPs are easily scaled. This research could motivate further exploration of GNR-based composites with other metal oxides, such as MnO$_2$ and Fe$_2$O$_3$, as anode materials for LIB applications.

EXPERIMENTAL SECTION

Preparation of Graphene Nanoribbons. The scalable production of GNRs was realized through the unzipping of multiwall carbon nanotubes (MWCNTs, Mitsui Chemicals).[21,22,37] Here, we employed the recently developed procedure to produce the conductive GNRs with good dispersibility in various organic solvents.[21] The synthesis is nearly identical to that previously described, only the scale was different. MWCNTs (100 mg, 8.3 mequiv C) were added to an oven-dried 250 mL round-bottom flask containing a magnetic stir bar. The vessel was then transferred to a N$_2$ glovebox where freshly distilled 1,2-dimethoxyethane (35 mL) and liquid Na/K alloy (0.29 mL) were added. Liquid Na/K alloy was made in a nitrogen glovebox by mixing freshly cut K (1 mol equiv) and Na (0.22 mol equiv) chunks. The flask with the suspension was then sealed with a septum and transferred out of the glovebox where it was dispersed by a short 5 min bath ultrasonication (Cole-Parmer model 08849-00) to yield a dark greenish to red suspension. After ultrasonication, the reaction mixture was vigorously stirred (450 rpm) at room temperature for 3 d. The reaction suspension was then quenched by the addition of methanol (20 mL, 500 mmol) using a syringe; stirring was continued at room temperature for 10 min. The reaction mixture was filtered over a 0.45 μm pore size PTFE membrane. The filter cake was successively washed with THF (100 mL), *i*-PrOH (100 mL), H$_2$O (100 mL), *i*-PrOH (20 mL), THF (20 mL), and Et$_2$O (10 mL). The filter cake was then dried under vacuum ($\sim$10^{-2} Torr) for 24 h to afford 124 mg of GNRs.

Synthesis of GNRs and SnO$_2$ NPs Composite. To an oven-dried 250 mL round-bottom flask containing a magnetic stir bar were added the GNRs (75 mg), together with SnCl$_2 \cdot$2H$_2$O (1.33 g, 5.89 mmol) and 2-pyrrolidinone (65 mL). The suspension was ultrasonicated for 20 min, followed by heating at reflux for 1 h. During this step, Sn^{2+} was reduced to Sn NPs, with partial intercalation into the GNR stacks. The reaction system was cooled to room temperature and ultrasonicated in the open air overnight to oxidize the Sn NPs to SnO$_2$. The reaction mixture was then quenched with acetone, and sequentially washed with acetone and water three times, then filtered over a 0.45 μm pore size PTFE membrane. The product was dried in a vacuum oven at 60 °C for 24 h, and finally annealed in a quartz tube furnace at 500 °C under an Ar atmosphere for 2 h to afford 380 mg of the GNRs/SnO$_2$ composite.

Assembly and Testing of Lithium Ion Batteries. Slurries were prepared by mixing 90% active material (GNRs/SnO$_2$ composite) and 10% sodium carboxymethyl cellulose (Na-CMC, Sigma Aldrich) binder with enough DI water to form a slurry; the amount of water varied with each active material and the precise amount did not impact the results. The control samples were prepared by mixing the SnO$_2$ with super carbon black. The working electrodes were made by coating 2–4 mg of slurry onto circular copper foil (25 μm-thick, Alfa Aesar) with diameters of 1.1 cm, and then dried overnight in the vacuum furnace (10 mTorr) at 120 °C under an Ar environment. Lithium foils (Sigma Aldrich) were polished in an Ar environment before use as both the counter and reference electrode. The working and counter electrodes were assembled in the glovebox (VAC, model: NEXUS) with controlled O$_2$ and H$_2$O levels <1 ppm. They were assembled into 2032 coin-type cells with a separator (Celgard 3501). One molar LiPF$_6$ in 1:1:1 (volume) ethylene carbonate:dimethyl carbonate:diethyl carbonate (MTI Corp.) was employed as electrolyte in the coin cells. The galvanostatic charge/discharge experiments were performed using MTI battery analyzers. The cyclic voltammetry (CV) measurements were carried out on a CHI 608D potentiostat/galvanostatic electrochemical station.

Supporting Information Available: Additional experimental details and electrochemical analysis graphs. This material is available free of charge *via* the Internet at http://pubs.acs.org.

REFERENCES AND NOTES

1. Armand, M.; Tarascon, J. M. Building Better Batteries. *Nature* **2008**, *451*, 652–657.
2. Whittingham, M. S. Lithium Batteries and Cathode Materials. *Chem. Rev.* **2004**, *104*, 4271–4301.
3. Buqa, H.; Goers, D.; Holzapfel, M.; Spahr, M. E.; Novak, P. High Rate Capability of Graphite Negative Electrodes for Lithium-Ion Batteries. *J. Electrochem. Soc.* **2005**, *152*, A474–A481.
4. Chan, C. K.; Peng, H. L.; Liu, G.; McIlwrath, K.; Zhang, X. F.; Huggins, R. A.; Cui, Y. High-Performance Lithium Battery Anodes Using Silicon Nanowires. *Nat. Nanotech.* **2008**, *3*, 31–35.
5. Derrien, G.; Hassoun, J.; Panero, S.; Scrosati, B. Nanostructured Sn-C Composite as an Advanced Anode Material in High-Performance Lithium-Ion Batteries. *Adv. Mater.* **2007**, *19*, 2336–2340.
6. Paek, S. M.; Yoo, E.; Honma, I. Enhanced Cyclic Performance and Lithium Storage Capacity of SnO$_2$/Graphene Nanoporous Electrodes with Three-Dimensionally Delaminated Flexible Structure. *Nano Lett.* **2009**, *9*, 72–75.
7. Fan, J.; Wang, T.; Yu, C. Z.; Tu, B.; Jiang, Z. Y.; Zhao, D. Y. Ordered, Nanostructured Tin-Based Oxides/Carbon Composite as the Negative-Electrode Material for Lithium-Ion Batteries. *Adv. Mater.* **2004**, *16*, 1432–1436.
8. Poizot, P.; Laruelle, S.; Grugeon, S.; Dupont, L.; Tarascon, J. M. Nano-Sized Transition-Metaloxides as Negative-Electrode Materials for Lithium-Ion Batteries. *Nature* **2000**, *407*, 496–499.
9. Hassoun, J.; Derrien, G.; Panero, S.; Scrosati, B. A Nanostructured Sn-C Composite Lithium Battery Electrode with Unique Stability and High Electrochemical Performance. *Adv. Mater.* **2008**, *20*, 3169–3175.
10. Liang, J. F.; Wei, W.; Zhong, D.; Yang, Q. L.; Li, L. D.; Guo, L. One-Step *in Situ* Synthesis of SnO$_2$/Graphene Nanocomposites and Its Application as an Anode Material for Li-Ion Batteries. *ACS Appl. Mater. Interfaces* **2012**, *4*, 454–459.
11. Zhu, X. J.; Zhu, Y. W.; Murali, S.; Stoller, M. D.; Ruoff, R. S. Reduced Graphene Oxide/Tin Oxide Composite as an Enhanced Anode Material for Lithium Ion Batteries Prepared by Homogenous Coprecipitation. *J. Power Sources* **2011**, *196*, 6473–6477.
12. Kim, H.; Kim, S. W.; Park, Y. U.; Gwon, H.; Seo, D. H.; Kim, Y.; Kang, K. SnO$_2$/Graphene Composite with High Lithium Storage Capability for Lithium Rechargeable Batteries. *Nano Res.* **2010**, *3*, 813–821.
13. Wen, Z. H.; Wang, Q.; Zhang, Q.; Li, J. H. *In Situ* Growth of Mesoporous SnO$_2$ on Multiwalled Carbon Nanotubes: A Novel Composite with Porous-Tube Structure as Anode for Lithium Batteries. *Adv. Funct. Mater.* **2007**, *17*, 2772–2778.
14. Wang, Y.; Zeng, H. C.; Lee, J. Y. Highly Reversible Lithium Storage in Porous SnO$_2$ Nanotubes with Coaxially Grown Carbon Nanotube Overlayers. *Adv. Mater.* **2006**, *18*, 645–649.
15. Berger, C.; Song, Z. M.; Li, X. B.; Wu, X. S.; Brown, N.; Naud, C.; Mayou, D.; Li, T. B.; Hass, J.; Marchenkov, A. N.; *et al.* Electronic Confinement and Coherence in Patterned Epitaxial Graphene. *Science* **2006**, *312*, 1191–1196.
16. Han, M. Y.; Ozyilmaz, B.; Zhang, Y. B.; Kim, P. Energy Band-Gap Engineering of Graphene Nanoribbons. *Phys. Rev. Lett.* **2007**, *98*, 206805-1-4.

17. Hod, O.; Barone, V.; Peralta, J. E.; Scuseria, G. E. Enhanced Half-Metallicity in Edge-Oxidized Zigzag Graphene Nanoribbons. *Nano Lett.* **2007**, *7*, 2295–2299.
18. Kudin, K. N. Zigzag Graphene Nanoribbons with Saturated Edges. *ACS Nano* **2008**, *2*, 516–522.
19. Uthaisar, C.; Barone, V.; Peralta, J. E. Lithium Adsorption on Zigzag Graphene Nanoribbons. *J. Appl. Phys.* **2009**, *106*, 113715–113715-6.
20. Bhardwaj, T.; Antic, A.; Pavan, B.; Barone, V.; Fahlman, B. D. Enhanced Electrochemical Lithium Storage by Graphene Nanoribbons. *J. Am. Chem. Soc.* **2010**, *132*, 12556–12558.
21. Genorio, B.; Lu, W.; Dimiev, A. M.; Zhu, Y.; Raji, A. R. O.; Novosel, B.; Alemany, L. B.; Tour, J. M. *In Situ* Intercalation Replacement and Selective Functionalization of Graphene Nanoribbon Stacks. *ACS Nano* **2012**, *6*, 4231–4240.
22. Kosynkin, D. V.; Lu, W.; Sinitskii, A.; Pera, G.; Sun, Z.; Tour, J. M. Highly Conductive Graphene Nanoribbons by Longitudinal Splitting of Carbon Nanotubes Using Potassium Vapor. *ACS Nano* **2011**, *5*, 968–974.
23. Cheng, B.; Russell, J. M.; Shi, W. S.; Zhang, L.; Samulski, E. T. Large-Scale, Solution-Phase Growth of Single-Crystalline SnO$_2$ Nanorods. *J. Am. Chem. Soc.* **2004**, *126*, 5972–5973.
24. Cullity, B. D.; Stock, S. R. *Elements of X-ray Diffraction*, 3rd ed.; Prentice Hall: Upper Saddle River, NJ, 2001.
25. Magasinski, A.; Zdyrko, B.; Kovalenko, I.; Hertzberg, B.; Burtovyy, R.; Huebner, C. F.; Fuller, T. F.; Luzinov, I.; Yushin, G. Toward Efficient Binders for Li-Ion Battery Si-Based Anodes: Polyacrylic Acid. *ACS Appl. Mater. Interfaces* **2010**, *2*, 3004–3010.
26. Chen, Z. H.; Christensen, L.; Dahn, J. R. Large-Volume-Change Electrodes for Li-Ion Batteries of Amorphous Alloy Particles Held by Elastomeric Tethers. *Electrochem. Commun.* **2003**, *5*, 919–923.
27. Li, J.; Lewis, R. B.; Dahn, J. R. Sodium Carboxymethyl Cellulose—a Potential Binder for Si Negative Electrodes for Li-Ion Batteries. *Electrochem. Solid-State Lett.* **2007**, *10*, A17–A20.
28. Chou, S. L.; Wang, J. Z.; Zhong, C.; Rahman, M. M.; Liu, H. K.; Dou, S. X. A Facile Route to Carbon-Coated SnO$_2$ Nanoparticles Combined with a New Binder for Enhanced Cyclability of Li-Ion Rechargeable Batteries. *Electrochim. Acta* **2009**, *54*, 7519–7524.
29. Mohamedi, M.; Lee, S. J.; Takahashi, D.; Nishizawa, M.; Itoh, T.; Uchida, I. Amorphous Tin Oxide Films: Preparation and Characterization as an Anode Active Material for Lithium Ion Batteries. *Electrochim. Acta* **2001**, *46*, 1161–1168.
30. Besenhard, J. O.; Winter, M.; Yang, J.; Biberacher, W. Filming Mechanism of Lithium-Carbon Anodes in Organic and Inorganic Electrolytes. *J. Power Sources* **1995**, *54*, 228–231.
31. Noerochim, L.; Wang, J. Z.; Chou, S. L.; Li, H. J.; Liu, H. K. SnO$_2$-Coated Multiwall Carbon Nanotube Composite Anode Materials for Rechargeable Lithium-Ion Batteries. *Electrochim. Acta* **2010**, *56*, 314–320.
32. Di Lupo, F.; Gerbaldi, C.; Meligrana, G.; Bodoardo, S.; Penazzi, N. Novel SnO$_2$/Mesoporous Carbon Spheres Composite Anode for Li-Ion Batteries. *Int. J. Electrochem. Sci.* **2011**, *6*, 3580–3593.
33. Demir-Cakan, R.; Hu, Y. S.; Antonietti, M.; Maier, J.; Titirici, M. M. Facile One-Pot Synthesis of Mesoporous SnO$_2$ Microspheres *via* Nanoparticles Assembly and Lithium Storage Properties. *Chem. Mater.* **2008**, *20*, 1227–1229.
34. Lian, P. C.; Zhu, X. F.; Liang, S. Z.; Li, Z.; Yang, W. S.; Wang, H. H. High Reversible Capacity of SnO$_2$/Graphene Nanocomposite as an Anode Material for Lithium-Ion Batteries. *Electrochim. Acta* **2011**, *56*, 4532–4539.
35. Yao, J.; Shen, X. P.; Wang, B.; Liu, H. K.; Wang, G. X. *In Situ* Chemical Synthesis of SnO$_2$-Graphene Nanocomposite as Anode Materials for Lithium-Ion Batteries. *Electrochem. Commun.* **2009**, *11*, 1849–1852.
36. Ji, L. W.; Lin, Z.; Alcoutlabi, M.; Zhang, X. W. Recent Developments in Nanostructured Anode Materials for Rechargeable Lithium-Ion Batteries. *Energy Environ. Sci.* **2011**, *4*, 2682–2699.
37. Kosynkin, D. V.; Higginbotham, A. L.; Sinitskii, A.; Lomeda, J. R.; Dimiev, A.; Price, B. K.; Tour, J. M. Longitudinal Unzipping of Carbon Nanotubes To Form Graphene Nanoribbons. *Nature* **2009**, *458*, 872–877.